

2019-12

Diverse sources of aeolian sediment revealed in an arid landscape in southeastern Iran using a modified Bayesian un-mixing model

Gholami, H

<http://hdl.handle.net/10026.1/15152>

10.1016/j.aeolia.2019.100547

Aeolian Research

Elsevier

All content in PEARL is protected by copyright law. Author manuscripts are made available in accordance with publisher policies. Please cite only the published version using the details provided on the item record or document. In the absence of an open licence (e.g. Creative Commons), permissions for further reuse of content should be sought from the publisher or author.

1 **Diverse sources of aeolian sediment revealed in an arid landscape in**
2 **southeastern Iran using a Bayesian un-mixing model**

3 **Abstract**

4 Identifying and quantifying source contributions of aeolian sediment is critical to mitigate
5 local and regional effects of wind erosion in the arid and semi-arid regions of the world. Sediment
6 fingerprinting techniques have great potential in quantifying the source contribution of sediments.
7 The purpose of this study is to demonstrate the effectiveness of fingerprinting methods in
8 determining the sources of the aeolian sands of a small erg with varied and complex potential
9 sources upwind. A two-stage statistical processes including a Kruskal-Wallis *H*-test and a stepwise
10 discriminant function analysis (DFA) were applied to select optimum composite fingerprints to
11 discriminate the potential sources of the aeolian sands from the Jazmurian plain located in Kerman
12 Province, southeastern Iran. A Bayesian un-mixing model was applied to quantify uncertainties
13 associate with the source contributions, and the model was evaluated by a goodness of fit (GOF)
14 method. The results suggest that four geochemical properties (Cr, Co, Ni, and Li) were the
15 optimum fingerprints for solving the Bayesian un-mixing model. The results show that there is
16 great diversity in terms of the sources of sand, and that, contrary to expectation, sediments
17 associated with an adjacent large ephemeral lake are the least significant in supplying sediment to
18 the erg. Sand-sheet-derived sands and alluvial sediments dominate a majority of the samples, and
19 are likely attributable to relatively short-distance aeolian flux, but substantial contributions from
20 alluvial fans and terraces likely represent longer distance pathways. These results highlight the
21 need to consider sediment provenance on a site-by-site basis. The GOF evaluation showed that
22 the Bayesian un-mixing model is an effective method to aid aeolian sediment fingerprinting. This
23 method may be applied to assess aeolian sediment sources in other desert regions with strong
24 aeolian activities.

25 **Key words:** Sediment Fingerprinting, Aeolian Sediment, Bayesian un-mixing Model,
26 Uncertainty, Jazmurian Plain.

27

28

30 **1. Introduction**

31 Desertification, or land degradation in the world's arid regions, is one of the world's most
32 pressing environmental issues (Dregne et al., 1991; UN, 2015). The United Nations Convention to
33 Combat Desertification (UNCCD, 1994) recognized several aspects of desertification leading to
34 the loss of productivity of dryland soils including aeolian and water erosion. Desertification
35 resulting from wind erosion and deposition, driven by changing climates (both drought and long-
36 term climate changes) and human activities has been reported in different climatic regions
37 worldwide (needs citations here). Drylands are typically highly susceptible to aeolian erosion and
38 land degradation, due to interactions between the typically sparse vegetation, lack of moisture to
39 bind the surficial sediments, and the susceptibility of the surface to disturbance and climate change
40 (Ravi *et al.*, 2010). In many arid and semi-arid regions, deflated sand accumulates in dune fields
41 (ergs), including parts of subtropical deserts and rain-shadowed zones of the mid-latitudes (Muhs,
42 2017). Although many studies have investigated aeolian dunes worldwide, much of the focus has
43 been on the dune initiation (Luna et al., 2011), sedimentary structures (Yang et al., 2018), and
44 palaeoclimatic implications of dated dune deposition (e.g. Lancaster et al., 2016; Thomas and
45 Burrough, 2013; Leighton et al., 2014; Li and Yang, 2015; Du and Wang, 2014). Very little
46 information is available on dune sediment provenance (Muhs, 2017), yet dune fields represent
47 potential archives of information in regional sediment transport pathways, as they are effectively
48 major sinks of the aeolian sediment regime.

49 Aeolian sediment transport fluxes in drylands are frequently complex, multi-directional and
50 may involve multiple sources, sinks and pathways. Furthermore, they are often intimately linked
51 to hydrological pathways, which themselves may operate only intermittently and unpredictably, in
52 the form of ephemeral drainages and lakes (playas) (Al-Masrahy & Mountney, 2015; Bullard &
53 Livingstone, 2002; Williams, 2015). Although terminal closed basins are often associated with
54 aeolian sediment emissions, often in the form of dust (e.g. Gill, 1996), other studies have
55 highlighted the role of dunefields as emission sources (Bullard *et al.*, 2008), and even alluvial fans
56 as sources of nearby dune sands (Howard *et al.*, 1999). Moreover, not all basins may contribute
57 equally as aeolian sources, perhaps most notably in the case of Saharan dust emissions, a
58 disproportionate amount of which is now known to originate from the Bodélé Depression in Chad

59 (Washington and Todd, 2005), and such emissions may also have complex spatio-temporal
60 dependency on localized hydrology (e.g. Dahmardeh Behrooz *et al.*, 2019). Therefore, identifying
61 sources of aeolian sediment and quantifying the contribution of different sources represent critical
62 steps for wind erosion control and management (Wang and Jia, 2013).

63 For the first time, Collins *et al.* (1997) applied a sediment fingerprinting method to quantify
64 contribution sources of fluvial sediments. Consequently, many researchers applied this technique
65 to quantify source contributions of fluvial sediments at various locations worldwide (e.g. Walling,
66 2005; Collins *et al.*, 2010; Zhang *et al.*, 2012; Smith and Blake, 2014; Le Gall *et al.*, 2017; Tiecher
67 *et al.*, 2018; Habibi *et al.*, 2019). Sediment fingerprinting is well-developed in the context of
68 fluvial sediments, but only recently has this approach has been introduced to quantifying source
69 contribution of aeolian sediments (Gholami *et al.*, 2017a, b; Liu *et al.*, 2016a; Wang *et al.*, 2017;
70 Dahmardeh Behrooz *et al.*, 2019). The successful development of sediment fingerprinting methods
71 for aeolian sediment deposits is important as it provides quantitative estimates of aeolian sediment
72 with constrained uncertainties which can be applied to diverse dryland regions and environmental
73 problems, especially where such transport fluxes may be complex and other methods of
74 provenancing (e.g. detrital zircon U-Pb dating) may be difficult to apply (Gholami *et al.*, 2017b).
75 The effectiveness of multiple composite fingerprints to quantify the provenance of aeolian
76 sediments reported by Liu *et al.*, (2016a) suggested that these methods could be useful in other
77 locations for studying provenance of aeolian sediments.

78 Geochemical characteristics of aeolian sediments deposited far from their source regions have
79 been used as proxies for their potential sources (Wang *et al.* 2017). Criteria to determine sources
80 are based on comparing the different geochemical properties of sediment samples and potential
81 source samples. In recent years, numerous different sediment fingerprinting techniques have been
82 developed to quantify sediment provenance, with hydrological applications most common at
83 present (Walling, 2013; Wang *et al.*, 2017). A wide range of properties have been employed in
84 sediment fingerprinting studies including geochemical elements (Collins *et al.*, 2012; Lamba *et al.*,
85 2015; Liu *et al.*, 2016a; Gholami *et al.*, 2017a; Gholami *et al.*, 2019), geochemical indicators (Vale
86 *et al.*, 2016), isotopic ratios (Douglas *et al.*, 1995), radionuclides (Walling *et al.*, 1999; Olley *et al.*,
87 2012), organic elements (Walling *et al.*, 1999; Gellis *et al.*, 2009), magnetic properties (Russell *et al.*,
88 *et al.*, 2001) and physical signatures (Kouhpeima *et al.*, 2010).

89 Results produced by sediment fingerprinting studies, however, may have various uncertainties
90 (Walling, 2013). In recent years, techniques such as Bayesian models and Monte Carlo simulation
91 were developed to evaluate uncertainties associate with sediment fingerprinting results (Collins et
92 al., 2012; Cooper et al., 2014; Pulley et al., 2015; Lamba et al., 2015; Liu et al., 2016b; Abban et
93 al., 2016; Cooper and Krueger, 2017; Nosrati et al., 2018; Habibi et al., 2019; Gholami et al.,
94 2019). However, most of these studies focused on fluvial systems and the application of these
95 modelling techniques to quantify source contribution of aeolian sediments is rare. Recently,
96 Gholami et al. (2017b) successfully applied a Bayesian mixing model to assess uncertainties
97 associated with results of aeolian sediment fingerprinting in the Yazd-Ardekan plain, Iran. Large
98 parts of Iran (an area of about 24 million ha) are arid or semi-arid areas where wind erosion acts
99 as an important geomorphological process over (Gholami et al., 2017a). About 25% of this area is
100 occupied by dune fields, including the Yazd, Ashkzar, Kashan and Jazmurian ergs (Figure 1).
101 Jazmurian erg and its surrounding areas at the southern border of Kerman and Sistan-Baluchestan
102 Provinces, Iran, experience severe wind erosion (Rashki et al, 2017). The aim of this research is
103 to test and evaluate the fingerprinting method to quantify sources of aeolian sediment in a dune
104 field with a complex potential range of sand sources (a large playa, associated terminal fluvial
105 channels, sand sheets and more distal alluvial fans), and to incorporate robust estimates of the
106 uncertainties associated with the fingerprinting results using a Bayesian un-mixing model.

107

108 **2. Material and methods**

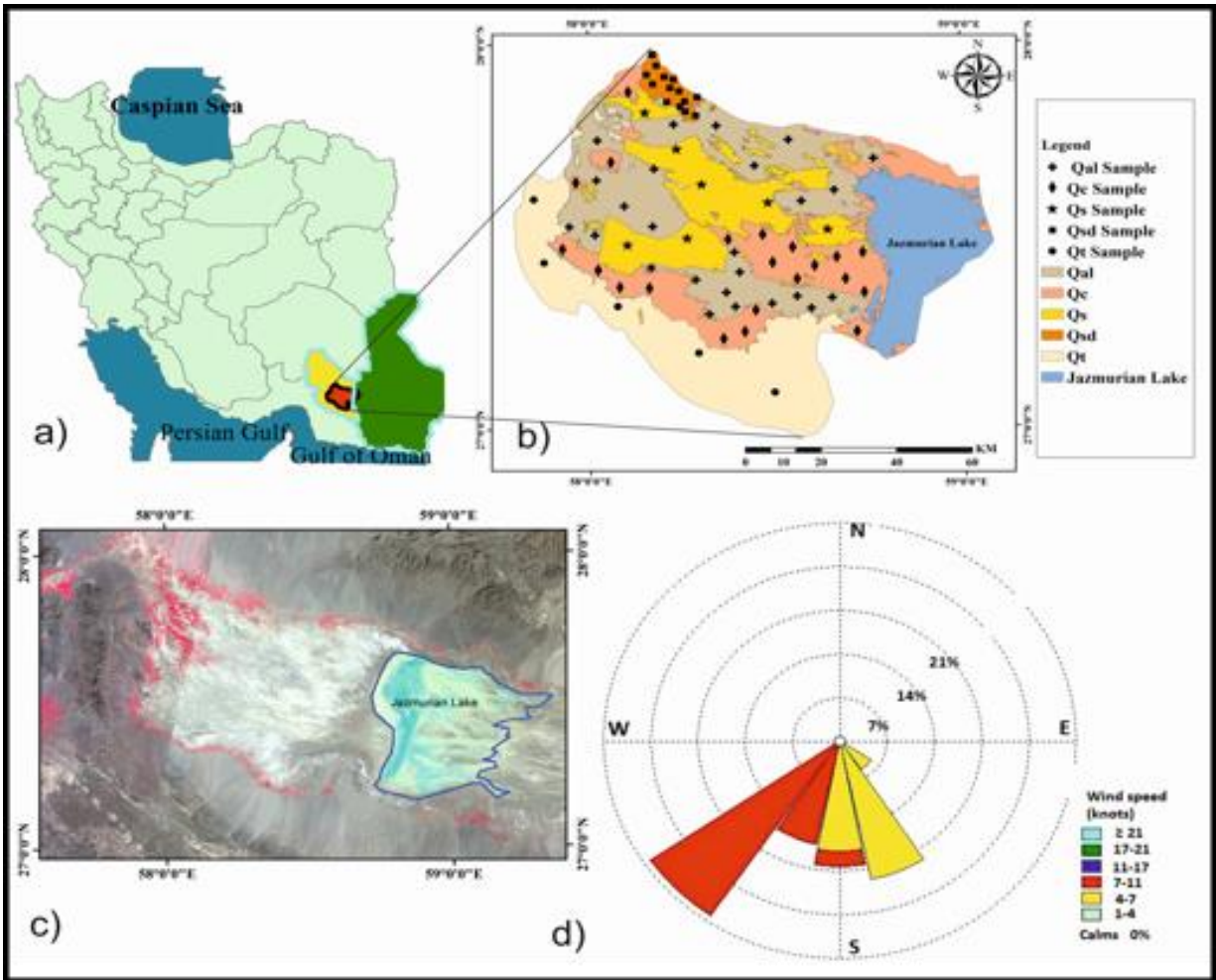
109 2.1 Study area

110 The study area is located in the Jazmurian Basin, in the Kerman Province of southeastern Iran
111 (Figure 1). With the Jabal Albarz mountains to the north, and separated from the Gulf of Oman
112 by the Makran mountains to the south, the Jazmurian Basin is a closed basin fed by the Bampur
113 River from the east, and the longer Halil (Haliri) River to the west. The region is arid, receiving
114 100-200 mm rainfall annually, but with evapotranspiration of up to 2500 mm year⁻¹ (Rashki,
115 Arjmand & Kaskaoutis, 2017). Geologically, this area is covered by five Quaternary geological
116 formations: (1) sand sheets (Q_s unit); (2) alluvial fine-grain sediments and dry river bed sediments
117 (Q_{al} unit); (3) alluvial fans and terraces (Q_t unit); (4) mixtures of clay and salt (the dried lake-bed
118 of Jazmurian lake, or Q_c unit) and (5) dune fields (Q_{sd} unit) (Figure 1, part B). The Q_s , Q_{al} , Q_t and
119 Q_c geological units are assumed to be the potential sources of aeolian sediments for the small erg

120 representing the deposition region, the Q_{sd} geological unit (Liu et al., 2016a; Gholami et al., 2017a,
121 b). The area of the case study is 8050 km² and it consists of 1754 km² Q_t unit, 1443 km² Q_s unit,
122 1667 km² Q_c unit, 1887 km² Q_{al} unit and 199 km² Q_{sd} unit.

123 Jazmurian lake covers, at its maximum extent, about 1100 km² of the study area, but the lake
124 is rarely inundated, and frequently completely dry; this has been the case since at least the earlier
125 half of the 20th century (Harrison, 1943). The lake has recently yielded sedimentological evidence
126 of palaeoclimatic change since the Last Glacial Maximum, revealing a complex aridity history,
127 with markedly wetter conditions during the early Holocene, with more minor excursions in
128 moisture availability throughout the last 20 ka (Vaezi *et al.*, 2019).

129 Dominant winds in the western Jazmurian region are mainly from the southwestern, southern
130 and southeastern directions (Figure 1, part E), though to the north and east they are more varied.
131 Extensive droughts in the early 2000s caused the Jazmurian lake to completely dry and resulted in
132 an increased frequency of dust events observed during 2001-2003. Dusty days in the Jazmurian
133 Basin ranged from 91 in 1996 to 203 in 2003 (Rashki et al., 2017). Increasing in frequency and
134 intensity of dust storms resulting from the desiccation of the lakes may raise serious problems for
135 the regional climate, ecosystems and human health (e.g. Rashki et al., 2013b). The Jazmurian
136 region is a main source of dust storms, and atmospheric dusts emitted from this area affect mostly
137 both sides of the Sea of Oman, including the southeastern Arabian Peninsula and western Pakistan
138 (Rashki et al., 2017).



139

140 **Figure 1.** Location and geological map of the Jazmurian region, south of Kerman, Iran and
 141 sampling sites. a) Location of study area (with red color) at the map of Iran and south of Kerman
 142 province (Yellow color); b) Geological map of study area. Different colors represent different
 143 geological sites in the study area; c) Landsat image (February 2017) of study area; and d) Annual
 144 wind rose from Kahnouj station. Number of sampling points = 72.

145

146 **2.2 Sampling and laboratory analysis**

147 A total of 72 sediment and soil samples were collected from the upper 0-5 cm depth of the
 148 potential sources and deposition regions (Figure 1, part B) in winter 2017. Among these samples,
 149 7 were collected from Q_s , 25 from Q_{al} , 5 from Q_t , 21 from Q_c source areas. Additionally, 14
 150 samples were collected from the dune fields (Q_{sd}) as aeolian sediments (Figure 1, part C). Source
 151 samples collected from points that were: (a) clearly derived from the geological unit; (b) within

152 the spatial coverage of the source area, broadly; and (c) influenced by wind erosion (Gholami et
153 al., 2017b).

154 The grain size distribution of the samples was determined using the dry sieve method. The
155 geochemical analysis of fingerprint properties focused on the 125- 410 μm fraction of the samples.
156 This is the predominant range of grain size in the aeolian sediment deposition area, and sediments
157 in this range are susceptible to aeolian transport (Field et al., 2010). The samples were digested
158 with aqua regia (Collins et al., 2012) and analyzed for Ni, Cu, Co, Cr, Ga, Mn, P, Ba, Sr and Li
159 using inductively coupled plasma optical emission spectroscopy (ICP-OES; Varian 730-ES
160 model). The relative standard deviation (% RSD), based on three replicates for each determinant
161 on each sample, was consistently $\leq 5\%$.

162 2.3 Potential sources of aeolian sediments

163 Selection of the optimum fingerprint involves quantitative assessment of the power of
164 individual properties to identify the potential sources of sediment (Collins et al., 2010). A two-
165 stage statistical procedure, which was introduced by Collins et al. (1997), was used to identify
166 optimum composite fingerprints to discriminate potential sources of aeolian sediments. At the first
167 step, the ability of potential sources' properties was investigated using the Kruskal-Wallis H test.
168 At the second step, optimum composite fingerprints were selected by a stepwise discriminant
169 function analysis (DFA). Wilks' lambda was used as the primary factor of discrimination in the
170 stepwise DFA, which determined the optimum fingerprints as input parameters to the model. This
171 two-stage procedure has been successfully applied by many studies for source fingerprinting of
172 fluvial sediments (Walling et al., 1999; Stone et al., 2014; Zhou et al., 2016; Chen et al., 2016; Liu
173 et al., 2016b) and more details of this method and its application to aeolian sediments may be
174 found in Gholami et al. (2017a, b).

175 2.4 Bayesian un-mixing model

176 In this study, we used a Bayesian un-mixing model, developed by Gholami et al. (2017b), to
177 quantify source contributions of aeolian sediments. It is a full Bayesian model in that all
178 hyperparameters are not fixed at a specific value and a prior distribution was selected for each
179 hyperparameter. Compared to an empirical Bayesian approach, a full Bayesian model is more
180 flexible and more complicated (Cooper et al., 2014). Further details of modelling procedure are

181 given in Gholami et al. (2017b) and Habibi et al. (2019). Compared to the model used in Gholami
 182 et al. (2017b) and Habibi et al. (2019), which used a Centered Log Ratio (CLR) transformation, in
 183 this study, we used the Dirichlet distribution for source contributions (Fox and Papanicolaou,
 184 2008). The Dirichlet distribution is a multivariate generalization of the beta distribution which
 185 satisfies the necessary boundaries constraints directly (that is, that all sources should sum to unity,
 186 and that all contribute between 0 and 1). It is thus simpler than the CLR transformation approach.

187 If $P = \{p_1, \dots, p_n\}$ follows the Dirichlet distribution with hyper-parameters $a_1, \dots, a_n > 0$, its
 188 density function is

$$189 \quad f(P) = \frac{\Gamma(\sum_{i=1}^n a_i)}{\prod_{i=1}^n \Gamma(a_i)} \prod_{i=1}^n p_i^{a_i-1} \quad (\text{eq. 1})$$

190 Here, $p_1, \dots, p_n \geq 0$ and $\sum_{i=1}^n p_i = 1$. Because there is no assumed prior information for the
 191 source contributions, we set hyper-parameters a_1, \dots, a_n equal to one. Similarly, in this study,
 192 weakly or non-informative hyper-parameters were used as prior distributions.

193 Because of the structure of the model, directly sampling from the Dirichlet distribution was
 194 not possible. Therefore, a beta distribution was used according to the following steps to sample
 195 $P = \{p_1, \dots, p_n\}$ values from Dirichlet distribution (Gelman et al., 2004). First using
 196 $Beta(a_1, \sum_{i=2}^k a_i)$ distribution p_1 was generated, then p_2, \dots, p_{n-1} were simulated using $p_j =$
 197 $(1 - \sum_{i=1}^{j-1} \theta_i) \phi_j$, where ϕ_j was sampled from $Beta(a_j, \sum_{i=j+1}^n a_i)$ distribution. Finally, p_n was
 198 calculated as $p_k = 1 - \sum_{i=1}^{n-1} p_i$.

199 It is not possible to obtain posterior distribution functions directly, as the joint posterior of all
 200 parameters is complex and high-dimensional. However, the Bayesian un-mixing model defined
 201 above can be analyzed using Markov Chain Monte Carlo (MCMC) modelling, and the parameters
 202 can be derived using the WinBUGS package (Lunn et al., 2000). The model was run 20,000,000
 203 times from the posterior distribution and the first 5,000,000 runs were considered as burn in. The
 204 model convergence during the runs was assessed by monitoring the trace plots of generated values
 205 (Gholami et al., 2017b).

206

207

208 2.5 Performance assessment of Bayesian un-mixing model

209 The goodness of fit (GOF) was used to evaluate the Bayesian un-mixing model performance
 210 according to Collins et al, (2012), and was calculated as follows:

$$211 \quad GOF = 1 - \frac{1}{n} * \sum_{i=1}^n \left[\frac{(B_i - \sum_{j=1}^m A_j \cdot X_{j,i})^2}{B_i} \right] \quad (eq. 2)$$

212 Where B_i indicates concentration of optimum fingerprint property (i) in the dune field samples;
 213 A_j is mean concentration of optimum fingerprint property (i) in source category (s); $X_{j,i}$ indicates
 214 optimized percentage contribution from potential source category (s); n is number of optimum
 215 fingerprints (in this research, $n=4$); and m is number of potential sources for dune field samples (in
 216 this study, $m=4$).

217 **3. Results**

218 3.1 Discrimination sources of aeolian sediments

219 Results of the two-stage statistical procedure are showed in Tables 1 and 2. Table 1 presents
 220 the results of the Kruskal-Wallis H -test, which was used to assess the ability of the tracer properties
 221 to discriminate the four potential sources including Q_s , Q_{ab} , Q_t and Q_c . The Kruskal-Wallis H -test
 222 (stage 1) showed that all of the 10 tracer properties could discriminate four potential sources at the
 223 99% level of confidence (Table 1).

224 **Table 1.** Kruskal-Wallis H -test results for selecting fingerprints to distinguish potential aeolian
 225 sediment sources in the Jazmurian plain.

Tracers	Ni	Cu	Co	Cr	Ga	Mn	P	Ba	Sr	Li
Chi-Square	40.9	40.6	39.3	40.8	40.2	34.4	39.3	18.3	39.7	41.7
Sig	0.00*	0.00*	0.00*	0.00*	0.00*	0.00*	0.00*	0.00*	0.00*	0.00*

226 * Statistically significant at $p < 0.01$

227 All tracer properties passing the Kruskal-Wallis H -test were entered to stepwise DFA as stage
 228 2 of the statistical verification. Table 2 shows that four optimum fingerprints were selected for
 229 modelling processes and to quantify source contribution of aeolian sediments. The four elements
 230 in question (Cr, Li, Ni and Co) are likely to reflect differing abilities to differentiate aspects of the
 231 region's complex geological past. Chromium is most likely associated with the Remeshk ophiolite

232 complex which lies unconformably to the south of the Jazmurian plain, whereas the commonly-
 233 associated nickel and cobalt are more likely attributable in origin to the metamorphic Deyader
 234 complex, also to the south (McCall, 2002). Lithium, meanwhile, is most abundant at the earth's
 235 surface as evaporite minerals associated with closed basins such as the Jazmurian plain, and its
 236 significance as a tracer probably relates to its ability to discriminate more local contributions.

237

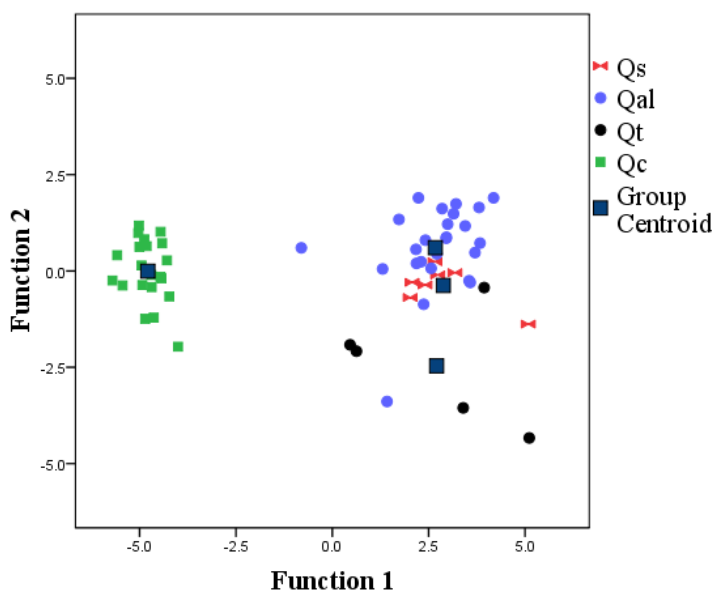
238 **Table 2.** Stepwise DFA results for selecting the optimum fingerprints.

Step	Optimum fingerprint	Wilks lambda	<i>p</i> -value
1	Cr	178.9	< 0.001
2	Li	55.1	< 0.001
3	Ni	37.8	< 0.001
4	Co	30.2	< 0.001

239

240 The stepwise DFA was able to correctly classify 81% of the variance between the potential
 241 source samples. Although stepwise DFA results suggested that good source discrimination was
 242 achieved, samples collected from Q_s shown slightly overlap with the Q_{al} source samples when the
 243 first and second functions were plotted (Figure 2).

244



245

246

247

248

249

250

251

252

253

254

255

256

257

258

259

260 **Figure 2.** Two-dimensional scatter plot constructed from the first and second discriminant
 261 functions calculated using the stepwise DFA in association with the stepwise selection of the
 262 optimum fingerprints for discriminating potential sources of aeolian sediments in the Jazmurian
 263 plain, south of Kerman, Iran. Scatter plot shows distribution of samples collected from four

264 potential sources including Q_s , Q_{al} , Q_t and Q_c in the Jazmurian Plain. The stepwise DFA selected
 265 four optimum fingerprints (Cr, Li, Ni and Co) that provided a good discrimination between
 266 potential sources with 81% samples correctly classified in the four sources.

267

268 3.2 Apportionment source of aeolian sediments by the Bayesian un-mixing model

269 Uncertainty ranges of main source contribution of aeolian sediments were estimated by the
 270 Bayesian un-mixing model with 95% confidence limits (Table 3, Figure 4). The Q_{al} unit (alluvial
 271 and dry river-bed sources) was recognized as the main source to supply materials for sediment
 272 samples 1, 2, 3 and 6, with mean contributions of 37%, 36%, 29%, and 36%, respectively. For
 273 sediment sample 4, Q_s is the main source with mean contributions of 29%. For sediment sample
 274 5, Q_t was recognized as main source and contribution ranged between 1-72% (with mean 29%).
 275 For sediment sample 7, about 33% of the materials came from the Q_{al} source (with contribution
 276 range 2-78%). The mean contributions from Q_s as main source for sediment samples 8, 9 and 10
 277 were 38% (with contribution range 2-82%); 35% (with contribution range 2-79%); and 27% (with
 278 contribution range 1-68%), respectively. For sediment samples 11 and 12, the Q_s was the main
 279 source and its contribution ranges were 2-78% (with mean 34%) and 1-73% (with mean 31%),
 280 respectively. For sediment samples 13 and 14, the Q_c was recognized as the main source and its
 281 contribution ranges were 6-65% (with mean 37%) and 7-64% (with mean 37%), respectively. In
 282 the Bayesian model, the MC errors for all of aeolian sediment samples were less than 0.1% (Table
 283 3), and the goodness of fit (GOF) values for 14 sediment samples ranged from 79% to 100%
 284 (Figure 3). The level of the MC error deviation is within the range proposed by Ntzoufras (2009).

285

286

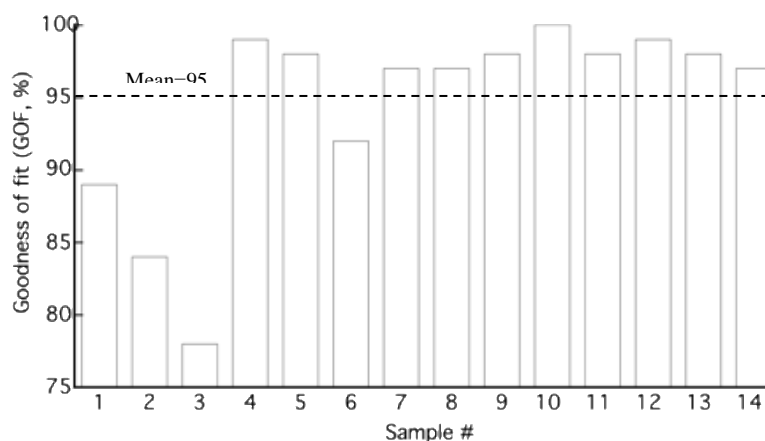
287

288

289

290

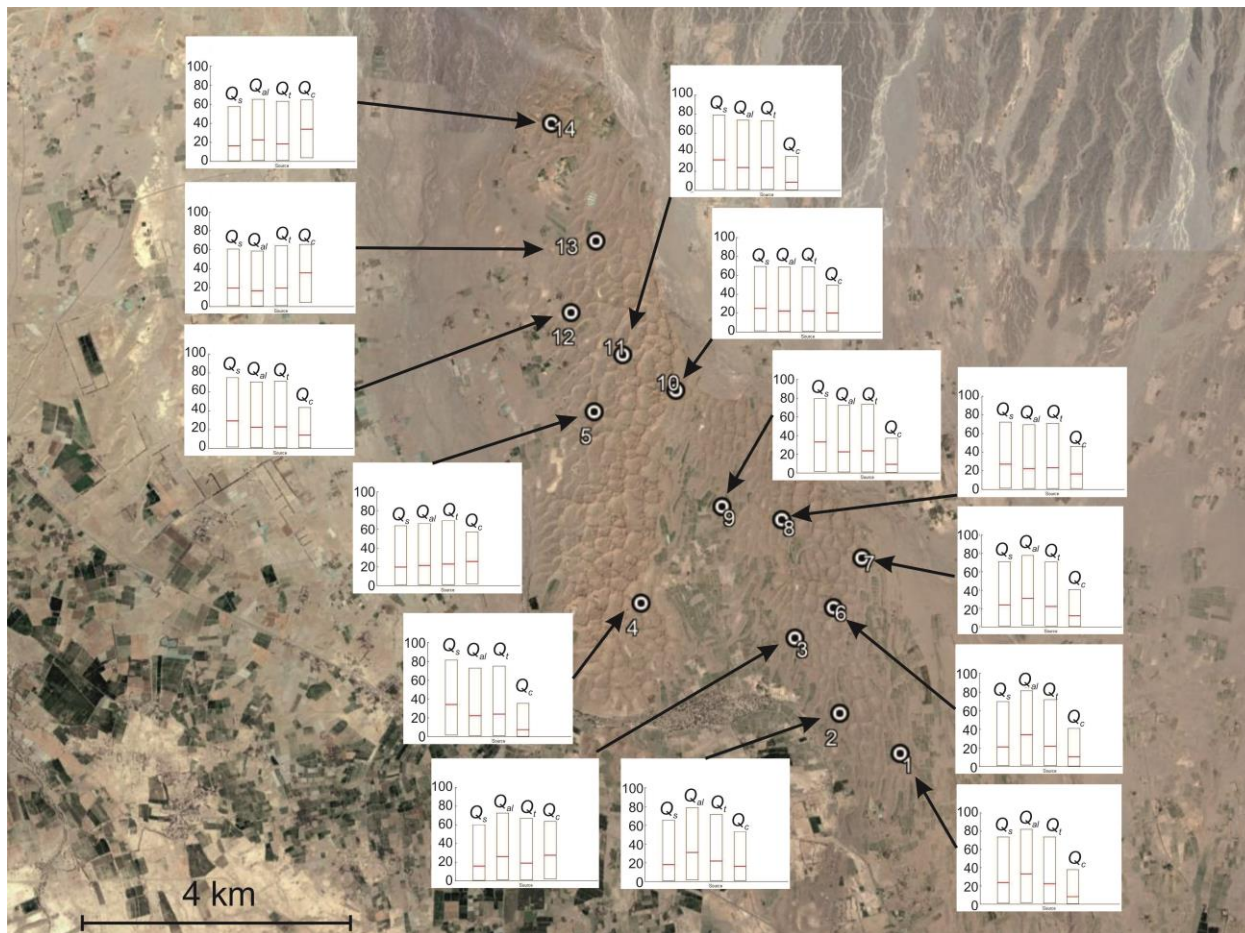
291



292

293 **Figure 3.** Goodness of fit (GOF) calculated for solutions of the Bayesian un-mixing model for the
294 aeolian sediment samples

295



296

297 **Figure 4.** Source contributions for the fourteen samples from Jazmurian erg, expressed as 95%
298 confidence intervals around a median. Note the general homogeneity of the sediment, with only
299 Jazmurian lake-bed sediments (Q_c) typically less common, although locally abundant; especially
300 in samples at the northern margin of the erg. Background imagery courtesy of Google Earth™.

301

302

303

304

305 **Table 3:** Uncertainty ranges (with 95% confidence limits) of source contributions for 14 aeolian
 306 sediment samples analyzed by the Bayesian un-mixing model.

Sediment	source	Mean %	Standard deviation	MC error ($\times 10^{-4}$)	2.5%	median	97.5%
1	Qs	27	0.20	3.03	1	23	74
	Qal	36	0.23	3.29	2	33	82
	Qt	26	0.20	2.91	1	22	73
	Qc	11	0.10	1.43	0	8	38
2	Qs	22	0.18	2.60	1	18	65
	Qal	33	0.22	3.19	1	31	79
	Qt	26	0.20	2.84	1	21	71
	Qc	19	0.14	2.08	1	16	53
3	Qs	20	0.16	2.32	1	16	60
	Qal	29	0.20	2.79	1	26	72
	Qt	23	0.18	2.53	1	19	67
	Qc	28	0.17	2.42	2	27	64
4	Qs	29	0.20	2.84	1	27	72
	Qal	26	0.19	2.58	1	22	69
	Qt	27	0.19	2.74	1	23	71
	Qc	18	0.12	1.70	1	16	46
5	Qs	23	0.17	2.45	1	20	64
	Qal	25	0.18	2.46	1	21	66
	Qt	26	0.19	2.54	1	23	69
	Qc	26	0.15	2.02	2	26	57
6	Qs	25	0.19	2.77	1	21	70
	Qal	36	0.23	3.23	2	34	81
	Qt	26	0.20	2.83	1	22	72
	Qc	13	0.11	1.58	0	10	41
7	Qs	27	0.19	2.79	1	24	71
	Qal	33	0.21	2.92	2	31	78
	Qt	26	0.19	2.73	1	22	71
	Qc	14	0.11	1.48	1	12	41
8	Qs	36	0.23	3.38	2	34	81
	Qal	26	0.20	2.83	1	22	73
	Qt	28	0.21	2.99	1	24	75
	Qc	10	0.10	1.27	0	7	35
9	Qs	35	0.22	2.97	2	33	80
	Qal	26	0.20	2.77	1	22	72
	Qt	27	0.20	2.77	1	23	73
	Qc	12	0.10	1.39	0	9	37
10	Qs	28	0.19	2.77	1	25	69

	Qal	25	0.19	2.69	1	22	68
	Qt	26	0.19	2.67	1	22	69
	Qc	21	0.13	1.92	1	20	50
11	Qs	34	0.22	3.13	1	32	79
	Qal	28	0.20	2.74	1	24	73
	Qt	27	0.20	2.79	1	24	73
	Qc	11	0.10	1.37	0	8	36
12	Qs	31	0.21	3.01	1	29	75
	Qal	26	0.19	2.85	1	22	70
	Qt	27	0.19	2.86	1	23	71
	Qc	16	0.11	1.64	1	14	43
13	Qs	22	0.16	2.31	1	20	61
	Qal	20	0.16	2.32	1	16	59
	Qt	23	0.17	2.37	1	19	64
	Qc	35	0.16	2.20	4	35	66
14	Qs	20	0.15	2.21	1	16	57
	Qal	25	0.18	2.62	1	22	65
	Qt	22	0.17	2.41	1	18	63
	Qc	33	0.16	2.26	4	34	64

307

308 4. Discussion

309 The results of our study show that the 10 tracer properties were able to identify aeolian
310 sediment sources at the 99% level of confidence. By using the stepwise discriminant function
311 analysis, the number of tracers was reduced to four (Cr, Co, Ni and Li), yet these can still explain
312 up to 81% of the variance between the sediment sources. Based on these four fingerprinting tracers,
313 we applied a Bayesian un-mixing model to identify the relative contribution of the four potential
314 sources to the aeolian sediment in the Jazmurian Plain, southeastern Iran. The performance of this
315 model, evaluated by using the GOF, ranged from 78% to 100%. The fact that a majority of the
316 GOF values was well above 80% suggested that the Bayesian model performed well in assessing
317 the sediment sources in our study area (Zhou et al., 2016; Haddadchi et al., 2013).

318 The results of this study are in sharp contrast to studies which identified both marked spatial
319 variability in the contributions of sources (e.g. Dahmardeh Behrooz *et al.*, 2019), and spatial
320 variability of provenance in depositional environments, even at a localized scale (Gholami et al
321 2017b). At Jazmurian, the sources of the aeolian sediment in our study area are very diverse and
322 no single source area had a contribution >40%. Desiccation of lakes in arid and semiarid areas

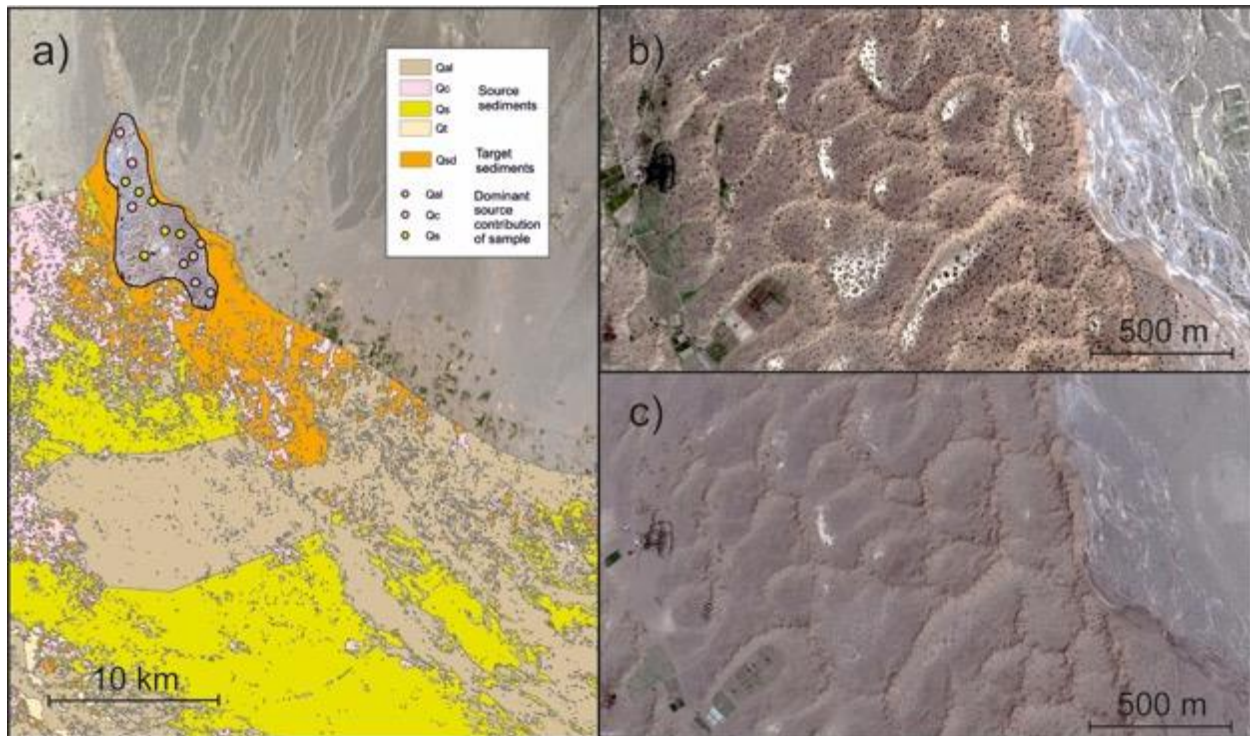
323 may affect the frequency and intensity of aeolian sediment transport at local to global scales, and
324 numerous studies have associated lake-beds with sources of aeolian emissions. These are reported
325 from locations as diverse as Owens Lake, USA (Reheis et al, 2009), Hamoun lakes, Iran (Rashki
326 et al, 2012; 2013a, b; Dahmardeh Behrooz et al., 2019), the Aral sea, Uzbekistan (Breckle et al,
327 2012), southern Africa (Prospero et al, 2002; and Mahowald et al, 2003), and Lake Eyre, Australia
328 (Baddock et al, 2009). Here, however, materials for only two or three sand field samples come
329 predominantly from the dried-bed of Jazmurian Lake (Q_c unit or mixture of clay and salt
330 materials), despite its extensive outcropping upwind of the erg (samples 13 and 14; sample 5 has
331 almost equal contributions from Q_c and Q_t).

332 Instead, this study shows the dunefield is supplied by a complex and diverse range of sources
333 (Figure 4), and that most samples, fluvial and alluvial sediments (Q_{al} unit), alluvial fan and terrace
334 sediments (Q_t unit), and sand sheets (Q_s unit), often contributing almost equally within the bounds
335 of uncertainty, are the predominant sources for twelve of the samples studied. Sediments from the
336 source area to Jazmurian erg are transported by winds that blow from the south and southeast
337 (Figure 1), where the sources are represented by a more proximal mixture of alluvial (Q_{al}), lake-
338 bed sediments (Q_c) and sand sheets (Q_s), with a more distal (~40 km) bajada of alluvial fans (Q_t)
339 bordering the Makran mountains to the south. Spatial patterning of sediment sources within the
340 dunefield sediment sources is limited (Figures 4 and 5), and only the sediment associated with the
341 Jazmurian lake units (Q_c) show strong variance, being more abundant at the northern/western end
342 of the erg. However, if the single largest mean contributions are considered (Figure 4), there is a
343 weak trend in the data for samples in the eastern edge of the erg to have alluvially-derived material
344 as the most abundant component, those to the center to have a more substantial component of sand-
345 sheet derived sediments, and only those to the west containing larger contributions of lake-bed
346 contributions. This observation likely reflects relatively local (km-scale) sediment sources and
347 pathways, as this pattern mirrors the nature of the substrate surrounding the erg, with outcropping
348 of lake-bed clays to the south-west, sand sheets to the south, and fluvial deposits to the south and
349 east (Figure 5a). However, the presence of a considerable alluvial fan (Q_t) component in all
350 samples probably highlights the importance of a longer-distance transport component, over scales
351 of 10 – 100 km (Figure 1), as local outcroppings of such deposits are very rare.

352 The aeolian sediment system in this region is a complex and interlinked interplay of sediment
353 pathways and stores, affected by periodic fluvial events, and not simply a case of sediment

354 deflating from an extensive ephemeral lake complex. Whilst the significance of dry fluvial and
355 alluvial materials as an aeolian sediment source is well reported (e.g. Cohen *et al.*, 2010; Du, Wu
356 & Tan, 2018), and Gholami *et al.*, (2017b) revealed that Quaternary alluvial fans and terraces
357 (alluvial sediments) are the main source of materials for sand fields in Yazd-Ardekan plain in
358 Central Iran. Here it is clear that almost all components of the landscape have the capacity for
359 aeolian sand mobilization at a range of scales. These findings are also in agreement with a recent
360 study by Ahmady-Birgani *et al.* (2018), which reported that simultaneous actions of alluvial,
361 fluvial and aeolian processes provide the majority of materials to the newly-formed sand fields
362 associated with the desiccation of Lake Urmia in northwestern Iran.

363 It is worth considering noting that the age of the dunes at Jazmurian erg is unknown, and that
364 absolute ages of Quaternary sediments from southern Iran are in general sparse. However, the
365 dunes remain active within recent years (Figure 5b and 5c), with at least surficial mobilization of
366 sands reshaping the surface of the dunes and interdunes. Where such longer records do exist, either
367 in terms of dated terrestrial sequences (Kehl, Frechen & Skowronek, 2005; Kehl, Frechen &
368 Skowronek, 2009; Rashidi *et al.*, 2019), or the recent lacustrine sequence from Jazmurian (Vaezi
369 *et al.*, 2019), they reveal multiple periods of varying climate during the Late Quaternary, with
370 likely periods of increased hydrological stress even during the Holocene. It is thus possible that
371 not all source areas contribute equally to the dunefield contemporaneously, and that changing wind
372 patterns on longer timescale may also contribute to the varied nature of the sands' origins.



373

374 **Figure 5.** Localized variance in the major source contributions to the sands of the dune field are
 375 likely associated with spatio-temporal variance in local sources. a) The dominant component of the
 376 target samples, whilst never markedly more than other contributions, does seem to relate to
 377 shorter distance transport with some east-west variance evident across the erg. b) The dune field's
 378 modern activity is evident by comparison with an image (courtesy of Google Earth™) from March
 379 2011, revealing bright interdunes, presumably rich with evaporites, with c) a comparable image
 380 from March 2012, showing the interdunes buried beneath blown sand. To the west of this image,
 381 fields are similarly covered, and dune crests in the southeast corner have moved on the order of
 382 ~10 m.

383

384 In terms of managing land degradation, this study highlights the potential for using sediment
 385 provenancing studies to better inform potential land management of aeolian desertification, and
 386 crucially, highlights the need to make such assessments on a site-by-site basis. The Jazmurian erg
 387 is adjacent to a large dryland lake system, which serves as the terminal basin for local hydrological
 388 activity across a sand-rich landscape, and which varies in extent on a range of timescales and is
 389 thus associated with extensive deposition of lacustrine sediments and evaporites. It might seem
 390 tempting to immediately ascribe that as the dominant source of aeolian sediments for Jazmurian
 391 erg (e.g., Gill, 1996). Yet establishing the provenance of the sediments of Jazmurian erg has
 392 revealed that the sands of the dunes are from a wide range of local sources, with substantial
 393 contributions from all major local landscape elements. This includes both short (km-scale) and

394 longer (10-100 km scale) contributions; focusing on managing the lake-bed's contribution would
395 be to overlook the majority of actual source material. Mitigation efforts to minimize aeolian
396 desertification at Jazmurian need to focus on a holistic approach to sand stabilization.

397 **5. Conclusions**

398 Sediment fingerprinting is an effective tool to quantify source contribution of aeolian
399 sediments. Results of our study show that aeolian, fluvial and alluvial processes are the main
400 sediment supplier's for dune fields in the Jazmurian plain of Iran. Like other modeling methods,
401 results produced by fingerprinting method are associated with uncertainties. Therefore,
402 quantifying uncertainty related to source contribution of aeolian sediment is essential for
403 environmental management. Here, we introduced a novel Bayesian un-mixing model to quantify
404 uncertainties associated with source contribution of aeolian sediments. The performance of the
405 revised model was satisfactory, as suggested by GOF.

406 Our study found that the sediment sources for the Jazmurian erg are diverse and likely
407 represent complex, multiphase sediment pathways, with evidence for sand transport at a range of
408 spatial scales. This finding, in contrast to other studies which have revealed sometimes singular
409 dominant landscape elements in terms of aeolian emissions, highlights the need investigate aeolian
410 transport pathways on a site-by-site basis, as there is marked spatial and temporal variability in the
411 consistency of sediment pathways. This knowledge can inform mitigation strategies for the
412 protection of agricultural and other land uses. The fingerprinting method and the uncertainty
413 evaluation approach proposed by this study has the potential to be applied to other arid and
414 semiarid systems, where aeolian sediment transport is a concern for aeolian desertification, air
415 quality, human health, and nutrient cycling.

416 **Conflict of Interest**

417 The authors declare that there is no conflict of interests regarding the publication of this
418 article.

419 **Acknowledgments**

420 The authors would like to thank the Faculty of Agriculture and Natural Resources, University
421 of Hormozgan, Iran, for supporting this joint research project.

422 **References**

- 423 Abban, B., Papanicolaou, A. N., Cowles, M. K., Wilson, C. G., Abaci, O., Wacha, K., Schilling,
424 K., and Schnobelen, D. (2016). An enhanced Bayesian fingerprinting framework for studying
425 sediment source dynamics in intensively managed landscapes. *Water Resource Research*, 52,
426 4646-4673. doi:10.1002/2015WR018030.
- 427 Ahmady-Birgani, H., Agahi, E., Ahmadi, S. J., and Erfanian, M. (2018). Sediment source
428 fingerprinting of the Lake Urmia Sand Dunes. *Scientific Reports*, 8:206, 1-15.
429 doi:10.1038/s41598-017-18027-0
- 430 Al-Masrahy, M. A. & Mountney, N. P. (2015) 'A classification scheme for fluvial–aeolian system
431 interaction in desert-margin settings'. *Aeolian Research*, 17 pp. 67-88.
- 432 Baddock, M. C., Bullard, J. E., and Bryant, R. G. (2009). Dust source identification using
433 MODIS: a comparison of techniques applied to the Lake Eyre Basin, Australia. *Remote Sens*
434 *Environ*, 113:1511–28.
- 435 Breckle, S.W., Wucherer, W., Liliya, A., Dimeyeva, L. A., Nathalia, P., and Ogar, N. P. (2012).
436 Aralkum - a man-made desert: the desiccated floor of the Aral Sea (Central Asia). Springer;
437 pp. 486.
- 438 Brewer, M. J., Filipe, J. A. N., Elston, D. A., Dawson, L. A., Mayes, R. W., Soulsby, Ch., and
439 Dunn, S. M. (2005). A Hierarchical Model for Compositional Data Analysis. *Journal of*
440 *Agricultural, Biological, and Environmental Statistics*, 10(1), 19–34.
441 doi:10.1198/108571105X28200
- 442 Bullard, J., Baddock, M., McTainsh, G. & Leys, J. (2008) 'Sub-basin scale dust source
443 geomorphology detected using MODIS'. *Geophysical Research Letters*, 35 (15),
444 Bullard, J. E. & Livingstone, I. (2002) 'Interactions between aeolian and fluvial systems in
445 dryland environments'. *Area*, 34 (1), pp. 8-16.
- 446 Chen, F., Fang, N., and Shi, Z. (2016). Using biomarkers as fingerprint properties to identify
447 sediment sources in a small catchment. *Science of the Total Environment*, 557-558, 123–133.
448 doi:10.1016/j.scitotenv.2016.03.028.
- 449 Cohen, T. J., Nanson, G. C., Larsen, J. R., Jones, B. G., Price, D. M., Coleman, M., and Pietsch,
450 T. J. (2010). Late Quaternary aeolian and fluvial interactions on the Cooper Creek Fan and
451 the association between linear and source-bordering dunes, Strzelecki Desert, Australia.
452 *Quaternary Science Reviews*, 29, 455-471.
- 453 Collins, A. L., Walling, D. E., and Leeks, G. J. L. (1997). Fingerprinting the origin of fluvial
454 suspended sediment in larger river basins: combining assessment of spatial provenance and
455 source type. *Geografiska Annaler*, 79, 239–254.
- 456 Collins, A. L., Zhang, Y., Walling, D. E., Grenfell, S. E., and Smith, P. (2010). Tracing sediment
457 loss from eroding farm tracks using a geochemical fingerprinting procedure combining local
458 and genetic algorithm optimisation. *Science of the Total Environment*, 408(22), 5461–5471.
459 doi:10.1016/j.scitotenv.2010.07.066
- 460 Collins, A. L., Zhang, Y., Walling, D. E., Grenfell, S. E., Smith, P., Grischeff, J., ... Brogden, D.
461 (2012). Quantifying fine-grained sediment sources in the River Axe Catchment, southwest
462 England: Application of a Monte-Carlo numerical modelling framework incorporating local
463 and genetic algorithm optimisation. *Hydrological Processes*, 26 (13), 1962–1983.
464 doi:10.1002/hyp.8283.
- 465 Cooper, R. J., and Krueger, T. (2017). An extended Bayesian sediment fingerprinting mixing
466 model for the full Bayes treatment of geochemical uncertainties. *Hydrological Processes*. doi:
467 10.1002/hyp.11154.

468 Cooper, R. J., Krueger, T., Hiscock, K. M., and Rawlins, B. G. (2014). Sensitivity of fluvial
469 sediment source apportionment to mixing model assumptions: A Bayesian model comparison.
470 *Water Resources Research*, 50: 9031-9047. doi:10.1002/2014WR016194.

471 Dahmardeh Behrooz, R., Gholami, H., Telfer, M. W., Jansen, J. D., and Fathabadi, A. (2019).
472 Using GLUE to pull apart the provenance of atmospheric dust. *Aeolian Research*, 37, 1-13.
473 <https://doi.org/10.1016/j.aeolia.2018.12.001>

474 Dong, Z. B., Chen, G. T., He, X. D., Han, Z. W. & Wang, X. M. (2004). Controlling blown sand
475 along the highway crossing the Taklimakan Desert. *Journal of Arid Environments*, 57 (3), pp.
476 329-344.

477 Douglas, G. B., Gray, C. M., Hart, B. T., and Beckett, R. (1995). A Strontium isotopic
478 investigation of the origin of suspended particulate matter (SPM) in the Murray-Darling river
479 system, Australia. *Geochimica et Cosmochimica Acta*, 59 (18), 3799-3815.
480 [https://doi.org/10.1016/0016-7037\(95\)00266-3](https://doi.org/10.1016/0016-7037(95)00266-3)

481 Dregne, H., Kassas, M., and Rozanov, B. (1991). A new assessment of the world status of
482 desertification. *J. Animal . Sci*, 69, 2463-2471.

483 Du, J. H., and Wang, X. L. (2014). Optically Stimulated Luminescence dating of sand-dune
484 formed within the Little Ice Age. *Journal of Asian Earth Sciences*.
485 <http://dx.doi.org/10.1016/j.jseaes.2014.05.012>

486 Du, S., Wu, Y., and Tan, L. (2018). Geochemical evidence for the provenance of aeolian deposits
487 in the Qaidam Basin, Tibetan Plateau. *Aeolian Research*, 32, 60-70.
488 <https://doi.org/10.1016/j.aeolia.2018.01.005>

489 Field, J. P., Belnap, J., Breshears, D. D., Neff, J. C., Okin, G. S., Whicker, J. J., Painter, T. H.,
490 Ravi, S., Reheis, M. C., and Reynolds, R. L. (2010). The ecology of dust. *Frontiers in Ecology*
491 *and the Environment*, 8(3); 423-430. <https://doi.org/10.1890/090050>

492 Fox, J. F., and Papanicolaou, A. N. (2008). An un-mixing model to study watershed erosion
493 processes. *Advances in Water Resources*, 31, 96–108. doi:10.1016/j.advwatres.2007.06.008

494 Gellis, A. C., Hupp, C. R., Pavich, M. J., Landwehr, J. M., Banks, W. S. L., Hubbard, B. E.,
495 Langland, M. J., Ritchie, J. C., and Reuter J. M. (2009). Sources, transport, and storage of
496 sediment in the Chesapeake Bay Watershed. U.S. Geological Survey Scientific Investigations
497 Report 2008-5186: 95.

498 Gelman, A., Carlin, J. B., Stern, H. S., and Rubin, D. B. (2004). *Bayesian Data Analysis*, 2nd
499 Ed., Chapman & Hall.

500 Gholami, H., Jafari TakhtiNajad, E., Collins, A.L., Fathabadi, A. (2019). Monte Carlo
501 fingerprinting of the terrestrial sources of different
502 particle size fractions of coastal sediment deposits using geochemical
503 tracers: some lessons for the user community. *Environ Sci Pollut Res*.
504 <https://doi.org/10.1007/s11356-019-04857-0>

505 Gholami, H., Middleton, N., NazariSamani, A. A., and Wasson, R. (2017a). Determining
506 contribution of sand dune potential sources using radionuclides, trace and major elements in
507 central Iran. *Arab J Geosci*, 10:163. doi. 10.1007/s12517-017-2917-0.

508 Gholami, H., Telfer, M. W., Blake, W. H., and Fathabadi, A. (2017b) Aeolian sediment
509 fingerprinting using a Bayesian mixing model. *Earth Surf. Process. Landforms*, doi:
510 10.1002/esp.4189.

511 Gill, T. E. (1996). Eolian sediments generated by anthropogenic disturbance of playas: human
512 impacts on the geomorphic system and geomorphic impacts on the human system.
513 *Geomorphology*, 17 pp. 207-228.

514 Habibi, S., Gholami, H., Fathabadi, A., and Jansen, J. D. (2019). Fingerprinting sources of
515 reservoir sediment via two modelling approaches. *Science of the Total Environment*, 663, 78-
516 96. <https://doi.org/10.1016/j.scitotenv.2019.01.327>

517 Haddadchi, A., Ryder, D., Evrard, O., and Olley, J. (2013). Sediment fingerprinting in fluvial
518 systems: review of tracers, sediment sources and mixing models. *International Journal of*
519 *Sediment Research*, 28, 560-578. doi.org/10.1016/S1001-6279(14)60013-5

520 Harrison, J. V. (1943) 'The Jaz Murian Depression, Persian Baluchistan'. *The Geographical*
521 *Journal*, 101 (5/6), pp. 206-225.

522 Howard, D. A., Ramsey, M. S., Christensen, P. R. & Lancaster, N. (1999) 'Identification of sand
523 sources and transport pathways at the Kelso Dunes, California, using thermal infrared remote
524 sensing'. *GSA Bulletin*, 111 (5), pp. 646-662.

525 Kehl, M., Frechen, M. & Skowronek, A. (2005) 'Paleosols derived from loess and loess-like
526 sediments in the Basin of Persepolis, Southern Iran'. *Quaternary International*, 140-141 pp.
527 135-149.

528 Kehl, M., Frechen, M. & Skowronek, A. (2009) 'Nature and age of Late Quaternary basin fill
529 deposits in the Basin of Persepolis/Southern Iran'. *Quaternary International*, 196 (1-2), pp.
530 57-70.

531 Kouhpeima, A., Feiznia, S., Ahmadi, H., Hashemi, S. A., and Zareiee, A. R. (2010). Application
532 of quantitative composite fingerprinting technique to identify the main sediment sources in
533 two small catchments of Iran. *Hydrology and Earth System Sciences*, 7, 6677–6698.
534 doi.org/10.5194/hessd-7-6677-2010

535 Lamba, J., Karthikeyan, K. G., and Thompson, A. M. (2015). Apportionment of suspended
536 sediment sources in an agricultural watershed using sediment fingerprinting. *Geoderma*, 239-
537 240, 25–33. doi:10.1016/j.geoderma.2014.09.024.

538 Lancaster, N., Wolfe, S., Thomas, D., Bristow, C., Bubbenzer, O., Burrough, S., Duller, G.,
539 Halfen, A., Hesse, P., Roskin, J., Singhvi, A., Tsoar, H., Tripaldi, A, Yang, X., and Zarate, M.
540 (2016). The INQUA Dunes Atlas chronologic database. *Quaternary International*, 410, 3-10.
541 <https://doi.org/10.1016/j.quaint.2015.10.044>

542 Le Gall, M., Evrard, O., Dapoigny, A., Tiecher, T., Zafar, M., Minella, J. P. G., Laceby, P., and
543 Ayrault, S. (2017). Tracing sediment sources in a subtropical agricultural catchment of
544 southern Brazil cultivated with conventional and conservation farming practices. *Land*
545 *Degradation and Development*, 28(4), 1426-1436. <https://doi.org/10.1002/ldr.2662>

546 Leighton, C. L., Thomas, D. S. G., and Bailey, R. M. (2014). Reproducibility and utility of dune
547 luminescence chronologies. *Earth Science Reviews*, 129, 24-39.
548 <http://dx.doi.org/10.1016/j.earscirev.2013.11.007>

549 Li, H., and Yang, X. (2015). Spatial and temporal patterns of aeolian activities in the desert belt
550 of northern China revealed by dune chronologies. *Quaternary International*, xxx, 1-11.
551 <http://dx.doi.org/10.1016/j.quaint.2015.07.015>

552 Liu, B., Niu, Q., Qu, J., and Zu, R. (2016a). Quantifying the provenance of aeolian sediments
553 using multiple composite fingerprints. *Aeolian Research*, 22, 117-122.
554 <dx.doi.org/10.1016/j.aeolia.2016.08.002>

555 Liu, B., Storm, D. E., Zhang, X. J., Cao, W., and Duan, X. (2016b). A new method for
556 fingerprinting sediment source contributions using distances from discriminant function
557 analysis. *Catena*, 147, 32–39. doi:10.1016/j.catena.2016.06.039.

558 Luna, M. C. M. de M., Parteli, E. J. R., Duran, O., and Herrmann, H. J. (2011). Model for the
559 genesis of coastal dune fields with vegetation. *Geomorphology*, 129, 215-224.
560 <https://doi.org/10.1016/j.geomorph.2011.01.024>

561 Lunn, D. J., Thomas, A., Best, N., and Spiegelhalter, D. (2000). WinBUGS - a Bayesian
562 modelling framework: concepts, structure, and extensibility. *Statistics and Computing*,
563 10:325--337.

564 Mahowald, N. M., Bryant, R. G., del Corral, J., and Steinberger, L. (2003). Ephemeral lakes and
565 desert dust sources. *Geophys Res Lett*, 30:1074. <http://dx.doi.org/10.1029/2002GL016041>

566 McCall, G. J. H. (2002). A summary of the geology of the Iranian Makran. Geological Society,
567 London, Special Publications, 195, 147.

568 Muhs, D. R. (2017). Evaluation of simple geochemical indicators of aeolian sand provenance:
569 Late Quaternary dune fields of North America revisited. *Quaternary Science Reviews*, 171,
570 260-296. doi.org/10.1016/j.quascirev.2017.07.007

571 Ntzoufras, I. (2009). Bayesian modelling using WinBUGS. John Wiley & Sons, Inc: Hoboken,
572 New Jersey.

573 Nosrati, K., Collins, A. L., and Madankan, M. (2018). Fingerprinting sub-basin spatial sediment
574 sources using different multivariate statistical techniques and the Modified MixSIR model.
575 *Catena*, 164, 32-43. <https://doi.org/10.1016/j.catena.2018.01.003>

576 Olley, J., Burton, J., Smolders, K., Pantus, F., and Pietsch, T. (2012). The application of fallout
577 radionuclides to determine the dominant erosion process in water supply catchments of
578 subtropical South-east Queensland, Australia. *Hydrological Processes*, 27(6), 885-
579 895. doi.10.1002/hyp.9422

580 Prospero, J. M., Ginoux, P., Torres, O., Nicholson, S. E., and Gill, T. E. (2002). Environmental
581 characterization of global sources of atmospheric soil dust identified with the Nimbus 7 total
582 ozone mapping spectrometer absorbing aerosol product. *Rev Geophys*, 40: 2–31

583 Pulley, S., Foster, I., and Antunes, P. (2015). The uncertainties associated with sediment
584 fingerprinting suspended and recently deposited fluvial sediment in the Nene River Basin.
585 *Geomorphology*, 228, 303–319. doi:10.1016/j.geomorph.2014.09.016.

586 Rashidi, Z., Sohbaty, R., Karimi, A., Farpoor, M. H., Khormali, F., Thompson, W. & Murray, A.
587 (2019) 'Constraining the timing of palaeosol development in Iranian arid environments using
588 OSL dating'. *Quaternary Geochronology*, 49 pp. 92-100.

589 Rashki, A., Arjmand, M., and Kaskaoutis, D. G. (2017). Assessment of dust activity and dust-
590 plume pathways over Jazmurian Basin, southeast Iran. *Aeolian Research*, 24, 145-160.
591 <http://dx.doi.org/10.1016/j.aeolia.2017.01.002>

592 Rashki, A., Eriksson, P. G., Rautenbach, C. J. D., Kaskaoutis, D. G., Grote, W., and Dykstra, J.
593 (2013a). Assessment of chemical and mineralogical characteristics of airborne dust in the
594 Sistan region, Iran. *Aeolian Research*, 90; 227-236.
595 <http://dx.doi.org/10.1016/j.chemosphere.2012.06.059>

596 Rashki, A., Kaskaoutis, D. G., Goudie, A. S., and Kahn, R. A. (2013b). Dryness of ephemeral
597 lakes and consequences for dust activity: The case of the Hamoun drainage basin, southeastern
598 Iran. *Science of the Total Environment*, 463-464; 552-564.
599 <http://dx.doi.org/10.1016/j.scitotenv.2013.06.045>

600 Rashki, A., Kaskaoutis, D. G., Rautenbach, C. J. D., Eriksson, P. G., Qiang, M., and Gupta, P.
601 (2012). Dust storms and their horizontal dust loading in the Sistan region, Iran. *Aeolian*
602 *Research*, 5; 51-62. doi:10.1016/j.aeolia.2011.12.001

603 Ravi, S., Breshears, D. D., Huxman, T. E., and D'odorico, P. (2010). Land degradation in

604 drylands: Interactions among hydrologic-aeolian erosion and vegetation dynamics.
605 *Geomorphology*, 116, 236-245.

606 Reheis, M., Budahn, J. R., Lamothe, P. J., and Reynolds, R. L. (2009). Compositions of modern
607 dust and surface sediments in the Desert Southwest United States. *J Geophys Res*, 114:
608 F01028. <http://dx.doi.org/10.1029/2008JF001009>

609 Russell, M. A., Walling, D. E., and Hodgkinson, R. A. (2001). Suspended sediment sources in
610 two small lowland agricultural catchments in the UK. *Journal of Hydrology*, 252, 1–24.
611 [doi.org/10.1016/S0022-1694\(01\)00388-2](http://dx.doi.org/10.1016/S0022-1694(01)00388-2)

612 Smith, H. G., and Blake, W. H. (2014). Sediment fingerprinting in agricultural catchments: A
613 critical re-examination of source discrimination and data corrections. *Geomorphology*, 204,
614 177–191. [doi:10.1016/j.geomorph.2013.08.003](http://dx.doi.org/10.1016/j.geomorph.2013.08.003).

615 Stone, M., Collins, A. L., Silins, U., Emelko, M. B., and Zhang, Y. S. (2014). The use of
616 composite fingerprints to quantify sediment sources in a wildfire impacted landscape, Alberta,
617 Canada. *Science of the Total Environment*, 473-474, 642–650.
618 [doi:10.1016/j.scitotenv.2013.12.052](http://dx.doi.org/10.1016/j.scitotenv.2013.12.052).

619 Thomas, D. S. G., and Burrough, S. L. (2013). Luminescence-based dune chronologies in
620 southern Africa: Analysis and interpretation of dune database records across the subcontinent.
621 *Quaternary International*, xxx, 1-16. <http://dx.doi.org/10.1016/j.quaint.2013.09.008>

622 Tiecher, T., Paolo, J., Minella, J. P. G., Evrard, O., Caner, L., Merten, G. H., Capoane, V.,
623 Didone, E. J., and dos Santos, D. R. (2018). Fingerprinting sediment sources in a large
624 agricultural catchment under no-tillage in southern Brazil (Conceicao river). *Land*
625 *Degradation and Development*. In press. <https://doi.org/10.1002/ldr.2917>

626 United Nations (2015). *Transforming Our World: The 2030 Agenda for Sustainable*
627 *Development*. New York: UN Publishing.

628 UNCCD, (1994). United Nations convention to combat desertification in those countries
629 experiencing serious drought and/or desertification, particularly in Africa (pp. 1–2). Geneva:
630 United Nations Environment Programme for the Convention to Combat
631 Desertification (CCD).

632 Vaezi, A., Ghazban, F., Tavakoli, V., Routh, J., Beni, A. N., Bianchi, T. S., Curtis, J. H. & Kylin,
633 H. (2019) 'A Late Pleistocene-Holocene multi-proxy record of climate variability in the
634 Jazmurian playa, southeastern Iran'. *Palaeogeography, Palaeoclimatology, Palaeoecology*,
635 514 pp. 754-767.

636 Vale, S. S., Fuller, I. C., Procter, J. N., Basher, L. R., and Smith, I. E. (2016). Characterization
637 and quantification of suspended sediment sources to the Manawatu River, New Zealand.
638 *Science of The Total Environment*, 543, 171–186. [doi:10.1016/j.scitotenv.2015.11.003](http://dx.doi.org/10.1016/j.scitotenv.2015.11.003)

639 Walling, D. E. (2005). Tracing suspended sediment sources in catchments and river systems.
640 *Science of the Total Environment*, 344 (1-3), 159–184. [doi:10.1016/j.scitotenv.2005.02.011](http://dx.doi.org/10.1016/j.scitotenv.2005.02.011).

641 Walling, D. E. (2013). The evolution of sediment source fingerprinting investigations in fluvial
642 systems. *Journal of Soils and Sediments*, 13 (10), 1658–1675. [doi:10.1007/s11368-013-0767-2](http://dx.doi.org/10.1007/s11368-013-0767-2).

643

644 Walling, D. E., Owens, P. N., and Leeks, G. J. L. (1999). Fingerprinting suspended sediment
645 sources in the catchment of the River Ouse, Yorkshire, UK. *Hydrological Processes*, 13, 955-
646 975. [doi. 10.1002/\(SICI\)1099-1085\(199905\)13:7<955::AID-HYP784>3.0.CO;2-G](http://dx.doi.org/10.1002/(SICI)1099-1085(199905)13:7<955::AID-HYP784>3.0.CO;2-G)

647 Wang, H. & Jia, X. (2013) Field observations of windblown sand and dust in the Takimakan
648 Desert, NW China, and insights into modern dust sources. *Land Degradation & Development*,
649 24 (4), pp. 323-333.

650 Wang, G., Li, J., Ravi, S., Scott Van Pelt, R., Costa, P. J. M., and Dukes, D. (2017). Tracer
651 techniques in aeolian research: approaches, applications, and challenges. *Earth-Sciences*
652 *Reviews*, 170, 1-16. <https://doi.org/10.1016/j.earscirev.2017.05.001>
653 Washington, R. & Todd, M. C. (2005) 'Atmospheric controls on mineral dust emission from the
654 Bodélé Depression, Chad: The role of the low level jet'. *Geophysical Research Letters*, 32
655 (17),
656 Williams, M. (2015) 'Interactions between fluvial and eolian geomorphic systems and processes:
657 Examples from the Sahara and Australia'. *CATENA*, 134 pp. 4-13.
658 Yang, L., Dong, Y., and Huang, D. (2018). Morphological response of coastal dunes to a group
659 of three typhoons on Pingtan Island, China. *Aeolian Research*, 32, 210-217.
660 <https://doi.org/10.1016/j.aeolia.2018.03.009>
661 Zhang, Y. S., Collins, A. L., and Horowitz, A. J. (2012). A preliminary assessment of the spatial
662 sources of contemporary suspended sediment in the Ohio River basin, United States, using
663 water quality data from the NASQAN program in a source tracing procedure. *Hydrological*
664 *Processes*, 26, 326-334. doi: 10.1002/hyp.8128
665 Zhou, H., Chang, W., and Zhang, L. (2016). Sediment sources in a small agricultural catchment:
666 A composite fingerprinting approach based on the selection of potential sources.
667 *Geomorphology*, 266, 11-19. [dx.doi.org/10.1016/j.geomorph.2016.05.007](https://doi.org/10.1016/j.geomorph.2016.05.007)
668